
Improving Visual Grounding by Encouraging Consistent Gradient-based Explanations

Ziyan Yang
Rice University
zy47@rice.edu

Kushal Kafle
Adobe Research
kkafle@adobe.com

Franck Deroncourt
Adobe Research
dernonco@adobe.com

Vicente Ordonez
Rice University
vicenteor@rice.edu

Abstract

We propose a margin-based loss for vision-language model pretraining that encourages gradient-based explanations that are consistent with region-level annotations. We refer to this objective as Attention Mask Consistency (AMC) and demonstrate that it produces superior visual grounding performance compared to models that rely instead on region-level annotations for explicitly training an object detector such as Faster R-CNN. AMC works by encouraging gradient-based explanation masks that focus their attention scores mostly within annotated regions of interest for images that contain such annotations. Particularly, a model trained with AMC on top of standard vision-language modeling objectives obtains a state-of-the-art accuracy of 86.59% in the Flickr30k visual grounding benchmark, an absolute improvement of 5.48% when compared to the best previous model. Our approach also performs exceedingly well on established benchmarks for referring expression comprehension and offers the added benefit by design of gradient-based explanations that better align with human annotations.

1 Introduction

Vision-language pretraining using images paired with captions has led to models that can transfer well to an array of tasks such as visual question answering, image-text retrieval and visual commonsense reasoning [29, 25, 8]. Remarkably, some of these models are also able to perform alignments between objects and phrases [30, 24, 12, 17] as demonstrated in benchmarks for visual grounding [35] and referring expression comprehension [21]. Some of the best performing models on visual grounding tasks however rely on a two-stage approach where first an object detector is trained on images annotated with labeled bounding boxes, and then a joint vision-language model is trained with the outputs of this object detector. This setup potentially limits two-stage methods by the quality and capabilities of the underlying object detectors used. Our work demonstrates that region and box annotations can be directly used in the vision-language model pretraining stage, thus bypassing the need for training object detectors. Moreover, our proposed approach demonstrates superior performance to two-stage methods while producing more explainable results.

Vision-language transformers extend the success of masked language modeling (MLM) based pretraining for NLP problems to multi-modal problems. In vision-language transformers, objectives such as image-text matching (ITM), and masked region prediction (MRM) are used in addition to MLM to account for the cross-modal nature of vision-language problems [25, 29, 8, 24]. We further extend these objectives to include our proposed attention mask consistency (AMC) objective. Our formulation is based on the observation that we can obtain gradient-based explanation maps using

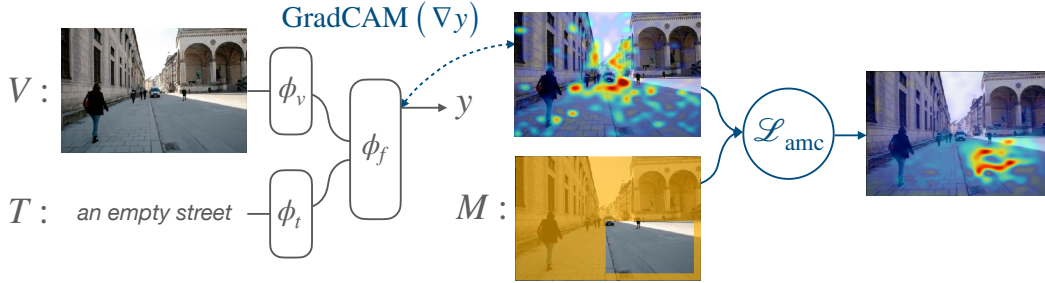


Figure 1: Overview of our method. Among other objectives, standard vision-language models are trained to produce a matching score y given an input image-text pair (V, T) as shown on the left. For inputs containing an extra level of supervision in the form of region annotations (e.g. a triplet (V, T, M)), we optimize the GradCAM [38] gradient-based explanations of the model so that the produced explanations are consistent with region annotations.

methods such as GradCAM [38] by relying on image-text matching objectives coupled with arbitrary text. Our AMC objective explicitly optimizes these explanations during training so that they are consistent with region annotations. Figure 1 shows a high level overview of our method.

The novelty of our work is twofold: First, we introduce a new training objective (AMC) and, secondly, at the conceptual level we demonstrate that box or region annotations can be leveraged jointly with image-text pretraining instead of training a separate model to explicitly predict locations. Our model establishes state-of-the-art accuracy in both visual grounding and referring expression comprehension for both methods that require object detectors and detector-free methods under a variety of settings. Our paper is organized as follows: Section 2 describes AMC in detail with a brief introduction to other standard training objectives, section 3 describes related work, section 4 describes our setup and experiments in detail. Our experiments include comparisons to both state-of-the-art and alternative training objectives.

2 Method

Vision-language pretraining consists of exploiting the structure of each input modality as well as their interactions. Our base model consists of three transformer encoders [42, 10]: An image encoder ϕ_v , a text encoder ϕ_t , and a multimodal fusion encoder ϕ_f . An input image V is encoded into a sequence of visual tokens $\{v_{cls}, v_1, v_2, \dots, v_n\}$ and the text encoder encodes the input text T as a sequence of tokens $\{t_{cls}, t_1, t_2, \dots, t_m\}$, where v_{cls} and t_{cls} are the embeddings of the [CLS] token for each transformer respectively. For each image-text pair drawn from a dataset $(V, T) \sim D$, a binary variable y represents whether the pair correspond with each other, i.e. whether the text actually describes the paired image. However, for some images a triplet $(V, T, M) \sim D$ might be available, where M additionally contains a region annotation, in the form of a binary mask, indicating the part of input image V that text T describes. In the following section we describe standard objectives used to capture intra-modality and inter-modality structure (Sec. 2.1), and then we describe our attention mask consistency objective (Sec. 2.2).

2.1 Standard Model Training Objectives

Masking Language Modeling (MLM) Originally introduced by BERT [10] in the context of language transformers, this objective has been adapted to multiple vision-language pretraining models such as [25, 29, 8] and is inspired by a long history in NLP of exploiting distributional semantics. The goal is to capture structure in the text by forcing the model to infer missing words from the input text. Each token in the input text is masked randomly with a small probability (usually 15%) and the model is then optimized to recover the masked tokens using information from both the remaining input text and the input image. Assume an input masked text is represented by T^{-m} , and the masked token is represented as a one-hot vector t^m , the objective will be expressed as:

$$\mathcal{L}_{mlm} = \mathbb{E}_{(V, T^{-m}) \sim D} H(t^m, \phi_f^m(\phi_v(V), \phi_t(T^{-m}))), \quad (1)$$

where $H(\cdot, \cdot)$ is the cross-entropy between the missing token t^m and a probability distribution over tokens output by a function ϕ_f^m which augments ϕ_f with a linear projection layer and softmax function over a corresponding output embedding. This objective is optimized over a large sample of choices for masked tokens and image-text pairs.

Image Text Matching (ITM) Another common objective inspired by BERT’s next sentence prediction objective, consists of image text matching. The purpose of this loss is to push the model to learn if a text and an image are matched. The output of the [CLS] token will be used to generate the output for this objective by adding a linear layer and a softmax activation function. We denote this entire operation as ϕ_f^{cls} . The objective is therefore defined as follows:

$$\mathcal{L}_{\text{itm}} = \mathbb{E}_{(V,T) \sim D} H(\mathbf{y}, \phi_f^{\text{cls}}(\phi_v(V), \phi_t(T))), \quad (2)$$

where \mathbf{y} is a one-hot vector with two entries $[y, 1 - y]$ indicating whether the drawn sample (V, T) corresponds to a matching image-text pair or not.

Image-Text Contrastive Loss (ITC) This objective has been useful in weakly supervised grounding [17, 24]. We follow ALBEF because it uses momentum distillation to potentially leverage a larger amount of negative image-text pairs. Assuming that each image-text pair is considered within a sample batch of K image-text pairs, this loss is defined as follows:

$$\mathcal{L}_{\text{itc}} = \mathbb{E}_{(V,T) \sim D} \frac{1}{2} \left[H\left(\mathbf{y}, s(V, T) / \sum_{k=1}^K s(V, T_k)\right) + H\left(\mathbf{y}, s(T, V) / \sum_{k=1}^K s(T, V_k)\right) \right], \quad (3)$$

where $s(V, T) = \exp(\phi_v(V) \cdot \phi_t(T) / \tau)$ computes the dot product between the output [CLS] token representations for the encoder transformer of each modality and τ is a temperature parameter, and $s(T, V)$ is defined similarly. The goal of this loss is to push for matching image-text pairs to have a closer representation than any non-matching image-text pair.

2.2 Attention Map Consistency (AMC)

In this section we explain in detail our proposed attention map consistency loss. Our proposed loss relies on first producing explanation heatmaps or “attention maps” using the GradCAM method [38]. In the context of vision-language transformers, this method can be used to highlight regions in the image that contribute to an image matching to an arbitrary input text, e.g., given an input image such as the one in Fig. 1, and an input text such as *an empty street*, we can generate a GradCAM visualization of areas in the input image that contribute to their matching score using \mathcal{L}_{itm} .

We assume that for a subset of images in our dataset we can obtain a triplet (V, T, M) where $M \in \{0, 1\}^2$ is a binary mask such that $M_{i,j}$ is 1 if the location i, j is inside region or 0 otherwise, V is the input image, and T is an input text describing region M . This assumption is generally fair in comparison to previous works that instead leverage images annotated with labels and bounding boxes to train an object detector. In our case, we can easily support this setup by turning a label annotation, e.g., dog into a region textual caption by prompt engineering, e.g., *an image of a dog*.

In order to compute a GradCAM heatmap, we first extract an intermediate feature map F_z in the multimodal fusion transformer ϕ_f and denote this function as ϕ_z :

$$F_z = \phi_z(\phi_v(V), \phi_t(T)). \quad (4)$$

Then, we calculate the gradient of F_z with respect to the matching loss \mathcal{L}_{itm} of this individual sample:

$$G_z = \nabla H(\mathbf{y}, \phi_f^{\text{cls}}(\phi_v(V), \phi_t(T))). \quad (5)$$

Next, we calculate a GradCAM attention heatmap A using F_z and G_z as follows:

$$A = \text{ReLU}(F_z \odot G_z), \quad (6)$$

where \odot is an element-wise multiplication. This heatmap is resized to the resolution of input images, and identifies which area in the image explains the model decision for its matching score.

The next step is to leverage the region annotations M so that the model focuses its heatmap scores in A inside the region of interest indicated by M . We first propose $\mathcal{L}_{\text{mean}}$ where we optimize a max

margin loss so that the mean value of the heatmap inside of the region of interest is larger than the mean value of the heatmap outside as follows:

$$\mathcal{L}_{\text{mean}} = \mathbb{E}_{(V,T,M) \sim D} \max \left(0, \frac{1}{N^c} \sum_{i,j} ((1 - M_{i,j}) A_{i,j}) - \frac{1}{N} \sum_{i,j} (M_{i,j} A_{i,j}) + \Delta_1 \right), \quad (7)$$

where Δ_1 is a margin term, and $N = \sum_{i,j} M_{i,j}$ is the number of locations inside the region of interest and N^c is the number of locations outside i.e. $\sum_{i,j} (1 - M_{i,j})$. This loss aims to ensure that the attention map A contains most of the scores inside the region M subject to this margin. We also propose to jointly maximize the margin between the largest score inside the region of interest M and the largest score outside the region of interest by a margin Δ_2 as follows:

$$\mathcal{L}_{\text{max}} = \mathbb{E}_{(V,T,M) \sim D} \max \left(0, \max_{i,j} ((1 - M_{i,j}) A_{i,j}) - \max_{i,j} (M_{i,j} A_{i,j}) + \Delta_2 \right). \quad (8)$$

Finally, we combine these two objectives:

$$\mathcal{L}_{\text{amc}} = \lambda_1 \cdot \mathcal{L}_{\text{mean}} + \lambda_2 \cdot \mathcal{L}_{\text{max}}, \quad (9)$$

where λ_1 and λ_2 are empirically determined weighting coefficients. We demonstrate in our experimental section that this objective effectively encourages model explanations that provide better grounding support for tasks such as referring expression comprehension and visual grounding.

3 Related Work

Vision-Language Representation Learning. Followed by the success of pretraining methods such as BERT [10], many transformer-based image-text models have been proposed to leverage benefits of pretraining on large-scale unlabeled image-text pairs [25, 26, 19]. While most earlier pretraining methods are built on top of existing object detection models, some recent works, such as ALBEF [24], have started using vision transformers such as ViT [11] directly, removing the hard-constraint and limitations of using object detectors. These pretrained models can then be finetuned to obtain impressive performance in a wide variety of vision-language tasks, such as image-text retrieval, visual question answering, visual commonsense reasoning and visual grounding. However object detector-based methods still provide advantages in grounding tasks where output locations are required. Our work builds a bridge between these two approaches.

Discriminative Localization. Localizing the most discriminative areas of an image for a given task has been widely used as a tool to provide visual explanation about a model. Class activation maps (CAM) [55] were proposed to provide weighted feature maps for any networks with minimal modifications to the model. Gradient-weighted Class Activation Mapping (GradCAM) [38] improves CAM by directly using gradients to obtain weighted feature maps without the need for model modifications or retraining; Grad-CAM++ [6] further explores the generalization of GradCAM by providing explanations for multiple objects in the same image on different visual tasks. The attention maps generated by these methods can be directly used as a source of weakly supervised localization. Our proposed method is also based on GradCAM heatmaps. However, instead of only using GradCAM during inference time, we use GradCAM during training to guide the generated heatmaps to achieve better consistency with known region and phrases that describe them. Recently, Pham et al [33] explore a similar idea by using segmentation masks to guide attention maps to focus on significant image regions for an attribute prediction task. Selvaraju et al [39] use saliency maps generated using Deep-USPS [31] at training time to guide attention maps in order to improve self-supervised representation learning. Similarly for self-supervised pre-training, Pillai et al [34] rely on consistent explanations for generic representation learning using contrastive objectives – leading to models with similar accuracy and better explanations. Our work, instead focuses on the weakly supervised setting but obtains models that are better at grounding compared to models trained with equal amounts of supervision and also obtains better gradient-based explanations.

Weakly Supervised Visual Grounding. Visual Grounding is a task that requires a model to select the region of an image described by a phrase. In weakly supervised visual grounding [28, 44, 17, 37, 49, 47, 7, 53, 14, 43, 16, 9, 48], the goal is to produce these predictions without directly training on annotated regions and phrases. Weakly supervised visual grounding methods can be broadly

grouped into two categories: First, methods that rely on the use of pretrained object detectors to extract features or generate box proposals for phrases [17, 28, 43]. These methods are limited by, and rely on the accuracy of object detectors for their predictions. The second group consists of models that are detector-free [3, 1, 20, 47, 52]. Our work does not use an object-detector to extract image features during training time, but the box annotations that are used to train these detectors are instead directly used as inputs to our model in the pretraining stage along with other standard objectives. Hence, our work contains properties of both detector-free and detector-based methods. In doing so, our method keeps the benefits of large-scale pretraining but gets rid of a hard-dependence on object detectors by involving box annotations directly, achieving higher quality and more accurate spatial heatmaps corresponding to phrases.

4 Experiments

In this section, we describe our pretraining setup and experimental evaluations. Our evaluations revolve around tasks that require pointing the location that an input text refers to in an image.

4.1 Training Details

Our model follows the architecture and training objectives of the ALBEF model [24] which uses the ALBEF-14M dataset as source of pretraining. ALBEF-14M is a large image-text data collection including the following datasets: COCO [27], Visual Genome (VG) [23] (excluding box annotations), SBU [32], CC3M [40] and CC12M [5]. In this data collection, each image is paired with one or several image descriptions so that we can sample pairs $(V, T) \sim D$. Additionally, several vision-language transformer models such as UNITER [8] or VisualBERT [25] further leverage box annotations from the Visual Genome dataset. We use this dataset as an additional source of triplets $(V, T, M) \sim D$. We start with the ALBEF model and further finetune it for 20 more epochs on Visual Genome with boxes using our proposed AMC loss. Next, we describe in detail how we leverage the Visual Genome dataset to produce triplets (V, T, M) in more detail.

First, we provide a more detailed description of the Visual Genome dataset. This dataset consists of 108,077 images and annotations in multiple formats such as boxes + region descriptions, boxes + object labels, and boxes + object attributes. At a first level, annotators of this dataset were asked to provide text that describes a region of the image and to provide a bounding box that covers the region. For instance, *a brown dog playing with a ball*. Then, the region descriptions were shown to other annotators that were asked to select objects from these regions and provide tight bounding boxes for selected objects and attributes e.g. *brown dog* and *ball*. Region bounding boxes and object+attribute bounding boxes are different for this dataset. The object detector trained by Anderson et al [2] on the object bounding boxes and object attributes of Visual Genome has been used by several previous weakly supervised visual grounding models. In order to compare fairly to these methods, we develop a model using the same training split as [2] and conduct our main experiments without the use of region descriptions. For completeness, we also conduct experiments using both objects with attributes and regions with descriptions.

We construct textual descriptions for object bounding boxes using prompt engineering templates. For example, if an image contains an object *dog* with an attribute *brown*, we construct the description as *a brown dog*. We filter out bounding boxes smaller than 8% of the whole image. To further increase the localization capabilities of our method, we further generate prompts with spatial references. For images with objects that correspond to more than one box, we select the leftmost/rightmost, top/bottom boxes and assign more detailed prompts such as *[obj] on the left*, *[obj] on the right*, *top [obj]* and *bottom [obj]*. Moreover, if the box falls into a corner of the image, we further assign them another level of spatial information such as *top left*, *top right*, *bottom left* and *bottom right*.

We conduct experiments on single node with 8 NVIDIA A40 GPUs. All experiments use a batch size of 512 and a learning rate of $1e-5$ with an Adam optimizer [22]. We determine empirically based on a small validation set two margin losses: $\Delta_1 = 0.1$ and $\Delta_2 = 0.5$ and determine our weighting coefficient for our losses as $\lambda_1 = 0.2$ and $\lambda_2 = 0.8$, respectively. For data augmentation, we resize images into a resolution of 256×256 and apply horizontal flips, color jittering and random grayscale conversions. We plan to open source our code to make the results fully reproducible and also include our code with this submission.

Method	Flickr30k	RefCOCO+		Method	Flickr30k	ReferIt
		test A	test B			
Align2Ground [9]	71.00	-	-	EB [52]	42.40	31.97
12-in-1 [30]	76.40	-	-	SSS [20]	49.10	39.98
InfoGround [17]	76.74	39.80	41.11	MG [1]	67.60	61.89
VMRM [12]	81.11	58.87	50.32	Gbs [3]	73.39	62.24
AMC†	86.49	78.89	61.16	ALBEF [24]	79.14	50.69
AMC*	86.59	80.34	64.55	AMC†	86.49	62.65
				AMC*	86.59	64.27

(a) Detector-based methods.

(b) Detector-free methods.

Table 1: Visual Grounding results using *pointing game* accuracy against the state-of-the-art. † indicates models only trained on boxes and box descriptions. * indicates models trained on both regions and boxes with descriptions.

4.2 Visual Grounding

Visual grounding consists in automatically associating an area of an image with an arbitrary piece of input text. A popular benchmark for this task is Flickr30k [35]. Since we are tackling the weakly supervised setting of this task, we only use the validation and testing splits. Each split includes a thousand images and is used for all of our model selections and evaluations. In Flickr30k Entities, each object phrase may pair with multiple ground truth boxes in the image. Our model will take the phrase and whole image as inputs, and find the most related regions corresponding to the phrase.

We report experimental results for Flickr30k Entities [35] with both detector-based and detector-free methods. *Pointing game* accuracy is a widely used metric in previous works for this task [17, 3, 44, 1], and we follow the same setting as in [1] to calculate this measure: After obtaining a heatmap given an input phrase and an image, we extract the position of the maximal point of this heatmap, and if this point falls in the target box, we count this result as positive. For detector-based methods, we follow [17] to calculate the *pointing game* accuracy by first ranking proposals generated by an object detector and then retaining one box proposal with highest score as the result. If the center point of the selected box proposal falls within the target box, this result is positive.

Our model trained with AMC achieves 86.49% accuracy on this task, and provides better performance than other detector-free methods (Table 1b) and models that use the same amount of supervision but train object detectors instead (Table 1a). Our model performs the best by a considerable margin. For Align2Ground [9] and 12-in-1 [30], we directly show the results reported in [3]. For InfoGround [17] and ALBEF [24], we use their provided trained models. For VMRM [12], since they do not provide their trained model, we re-train it using the official code and their used features and boxes from MMF [41] and MAF [45]. Align2Ground, 12-in-1 and VMRM all use image features generated by object detectors trained on VG boxes and attributes [2]. InfoGround uses image features extracted from an object detector trained on VG boxes. Results for EB [52], SSS [20], MG [1] and Gbs [3] are taken from their papers directly. Both MG and Gbs results reported here are obtained from models trained on VG. Qualitative results for GradCAM explanations are presented in Figure 2 for three input images with three input phrases for our model and for two other vision-language transformers. We observe that our model trained with AMC produces explanations that align better with true referents.

4.3 Referring Expression Resolution

Referring expressions are textual descriptions that refer unambiguously to an object or region of an image. Users are explicitly prompted to write a textual description to refer to a specific object. However the setup is similar to the visual grounding setup and as such, many previous methods compare their results across both benchmarks. We adopt the same *pointing game* accuracy metric and compare our results against previous methods in two benchmark datasets: RefCOCO+ [50, 21] and ReferIt [21]. We compare against the same set of methods as in the visual grounding task except

Method	Overall	People	Animals	Vehicles	Instrum.	Bodyparts	Clothing	Scene	Other
EB [52]	42.4	-	-	-	-	-	-	-	-
SSS [20]	49.1	-	-	-	-	-	-	-	-
MG(VGG) [1]	61.7	67.3	86.7	78.1	28.6	40.8	47.2	68.5	50.2
MG(PNAS) [1]	69.2	75.6	87.6	83.8	57.5	44.9	58.3	68.2	59.8
Gbs(VGG) [3]	72.6	82.5	91.5	81.1	56.6	34.8	58.6	70.9	59.9
Gbs(PNAS) [3]	74.5	83.6	89.3	92.1	83.3	53.2	50.1	71.3	66.7
ALBEF [24]	79.1	80.1	89.8	89.8	83.3	63.3	85.5	83.8	70.2
Align2Ground [9]	71.0	-	-	-	-	-	-	-	-
12-in-1 [30]	76.4	85.7	82.7	95.5	77.4	33.3	54.6	80.7	70.6
InfoGround [17]	76.7	83.2	89.7	87.0	69.7	45.1	74.5	80.6	67.3
VMRM [12]	81.1	88.0	92.3	94.3	66.7	55.1	79.8	85.1	69.9
AMC	86.6	89.7	95.2	93.8	86.4	69.8	89.0	91.4	77.7

Table 2: We compare our method with previous detector-based and detector-free methods on Flickr30k Entities dataset for all the categories by reporting pointing game accuracy.

for Align2Ground [9] and 12-in-1 [30] which do not provide results for RefCOCO+. Additionally, InfoGround [17] does not report results for RefCOCO+, therefore, we use their provided bounding boxes for COCO images [27] to perform this evaluation.

We describe in more detail each benchmark. RefCOCO+ [50] is a widely used referring expression dataset including 20K images from the COCO dataset [27]. The expressions in RefCOCO+ were collected so that they do not allow words such as *left* or *right*, making it slightly more challenging. From this dataset, we only use its validation and testing splits. The testing split of this dataset is further divided into two subsets: *test A* and *test B*, in which the former only includes people as the target objects and the latter includes all objects. The total number of testing images is 1.5K. The ReferIt dataset [21] was collected based on the ImageCLEF IAPR dataset [15] and the SAIAPR TC-12 expansion data [13]. The expressions in this dataset include many positional words such as *on the left*, *to the right*, *above* and *below*. We use the same validation and testing splits as Akbari et al [1] which include 1K validation images and 10K testing images.

Tables 1b and 1a show results for referring expression resolution along with visual grounding for both detector-free and detector-based methods. Our work shows state-of-the-art accuracy in all these benchmarks. In general, we find detector-based methods do not perform very well on RefCOCO+ because this dataset provides phrases describing a specific object on the image without any context. Furthermore, when these methods use object detectors to extract box features, both image and description context information are lost.

4.4 Discussion of Results

In general, we see that the previous detector-free methods cannot perform as well as detector-based methods on Flickr30k Entities. Our method obtains 86.59%, which is 13.2% higher than Gbs, a detector-free model. We also observe that ALBEF [24] can only obtain 50.69% on the ReferIt benchmark, because descriptions in this dataset involve many direct spatial information words such as *left* and *right* and ALBEF does not have such explicit spatial information during training. In contrast, our method provides spatial information from both boxes and descriptions, improving the accuracy to 64.27%, which is better than the 62.24% obtained by Gbs. If we use only box descriptions, we can still achieve 62.65%, which is comparable with the results obtained by Gbs.

We report more fine-grained results comparing both detector-based and detector-free methods with our method in Table 2 for Flickr30K Entities. There are eight categories in this dataset. We evaluate on each category and report the pointing game accuracy for them separately. For MG and Gbs, we report results when trained on COCO because their models achieved their best performances on Flickr30k Entities under this setting. In general, our method obtains better results for almost all

Data	Flickr30k	ReferIt	RefCOCO+		Loss	Flickr30k	ReferIt	RefCOCO+	
			test A	test B				test A	test B
box	86.49	62.65	78.89	61.16	$\mathcal{L}_{\text{cosine}}$	84.85	61.21	76.41	60.81
region	85.14	59.16	77.89	61.26	$\mathcal{L}_{\text{mean}}$	82.83	57.63	75.34	56.90
both	86.59	64.27	80.34	64.55	\mathcal{L}_{max}	86.56	62.79	80.34	64.47
					\mathcal{L}_{amc}	86.59	64.27	80.34	64.55

(a) Data Variations

(b) Loss Variations

Table 3: We conduct an ablation study to evaluate effectiveness of two components in our method. The type of supervision we use and the choices we made in our AMC training objective.



Figure 2: Qualitative comparison of the generated explanations for various images and input phrases. First column: original images from Flickr30k Entities; in each colored area from left to right: bounding boxes selected by VMRM; heatmaps generated by ALBEF; heatmaps generated by our method. On the top of each group of images, we show the caption and target phrases.

the categories and reaches 86.6% for all the testing samples. For the category *vehicle* our method obtains 93.8%, which is only 1.7% lower than the best result from the best method (12-in-1).

In Figure 2 we show and compare visual explanations obtained by our model against those obtained by VMRM [12] and GradCAM heatmaps generated by ALBEF. The text input for VMRM is the whole caption and a phrase and it produces a bounding box prediction. The model locates the positions of the phrase in the caption and selects boxes corresponding to the phrase with context information. For ALBEF and our method, the text input is only a phrase. We found our method can get more accurate and more complete objects from phrases. For example, in the last row, our method can provide a more precise heatmap for the referred object for *traditional asian clothing* than ALBEF, and in this case, VMRM is confused by the clothing from the woman instead of the boy. Additionally, in the second row, when the model is asked to find “the guitar”, our method can accurately cover the guitar, but ALBEF covers several unrelated regions that probably contribute to the detection of guitar but do not provide an explanation that aligns with what a human would annotate for this image.

4.5 Ablation Studies

In this section, we present ablations and variants of our model and training setup.

Data Variant. As described in section 4.1, VG [23] includes regions with descriptions and objects with attributes. We evaluate our method on each separately. For Flickr30k Entities and ReferIt datasets, boxes with generated descriptions using attributes lead to better results than regions with descriptions. We believe this is caused by accurate localization information provided by boxes and spatial information from box descriptions. For RefCOCO+ test B, regions with descriptions perform slightly better than boxes with attributes. By combining boxes, regions and two kinds of descriptions, we obtain better alignment between phrases and image subareas. Our full set of results are in Table 3a.

Loss Variant. Instead of calculating our margin loss as in Eq. 9, we calculate and minimize the cosine distance between M and A . Therefore, the generated heatmap will be closer to the box mask. Results combining both box and region information in VG are shown in Table 3b. For all datasets, our method outperforms this cosine distance loss $\mathcal{L}_{\text{cosine}}$, proving our method is a better way to use box information than more trivial dot product optimizations. Furthermore, we evaluate two components in Eq. 9: $\mathcal{L}_{\text{mean}}$ and \mathcal{L}_{max} . We find \mathcal{L}_{max} is very significant in AMC, but $\mathcal{L}_{\text{mean}}$ also provides complementary information, especially for the ReferIt dataset. In general, combining two terms leads to a more comprehensive grounding ability.

5 Conclusion

In this paper, we proposed Attention Map Consistency (AMC). From the intuition that a model should focus on meaningful regions guided by location information, we reuse the bounding boxes which are usually used to train object detectors to extract better image features for similar tasks. Our approach efficiently involves the location information during training to guide the attention of the multimodal transformer model and achieves new state-of-the-art results on multiple visual grounding datasets with weak supervision.

6 Broader Impacts and Limitations

Our model relies on some pretraining data that was filtered through automatic means. For instance, SBU [32], and CC12M [5]. Relying on this type of large automatically collected data might expose the model to learning societal biases from large scale data as evidenced and discussed in prior work [54, 46, 4]. Responsible deployment of this type of models would have to balance the risk and opportunities of using this type of model and further curate the sources of training before deployment. In terms of limitations, our work is still limited by the amount of training data available. Region annotations are more expensive to produce than image-level labels. While our method did show how far it is possible to improve accuracy with a modest amount of region-level supervision, it is still an open question how to scale these type of methods in the self-supervised setting.

References

- [1] Hassan Akbari, Svebor Karaman, Surabhi Bhargava, Brian Chen, Carl Vondrick, and Shih-Fu Chang. Multi-level multimodal common semantic space for image-phrase grounding. In *Proceedings of the IEEE/CVF Conference on Computer Vision and Pattern Recognition*, pages 12476–12486, 2019.
- [2] Peter Anderson, Xiaodong He, Chris Buehler, Damien Teney, Mark Johnson, Stephen Gould, and Lei Zhang. Bottom-up and top-down attention for image captioning and visual question answering. In *Proceedings of the IEEE conference on computer vision and pattern recognition*, pages 6077–6086, 2018.
- [3] Assaf Arbelle, Sivan Doveh, Amit Alfassy, Joseph Shtok, Guy Lev, Eli Schwartz, Hilde Kuehne, Hila Barak Levi, Prasanna Sattigeri, Rameswar Panda, et al. Detector-free weakly supervised grounding by separation. In *Proceedings of the IEEE/CVF International Conference on Computer Vision*, pages 1801–1812, 2021.

- [4] Rishi Bommasani, Drew A Hudson, Ehsan Adeli, Russ Altman, Simran Arora, Sydney von Arx, Michael S Bernstein, Jeannette Bohg, Antoine Bosselut, Emma Brunskill, et al. On the opportunities and risks of foundation models. *arXiv preprint arXiv:2108.07258*, 2021.
- [5] Soravit Changpinyo, Piyush Sharma, Nan Ding, and Radu Soricut. Conceptual 12m: Pushing web-scale image-text pre-training to recognize long-tail visual concepts. In *Proceedings of the IEEE/CVF Conference on Computer Vision and Pattern Recognition*, pages 3558–3568, 2021.
- [6] Aditya Chattopadhyay, Anirban Sarkar, Prantik Howlader, and Vineeth N Balasubramanian. Grad-cam++: Generalized gradient-based visual explanations for deep convolutional networks. In *2018 IEEE winter conference on applications of computer vision (WACV)*, pages 839–847. IEEE, 2018.
- [7] Kan Chen, Jiyang Gao, and Ram Nevatia. Knowledge aided consistency for weakly supervised phrase grounding. In *Proceedings of the IEEE Conference on Computer Vision and Pattern Recognition*, pages 4042–4050, 2018.
- [8] Yen-Chun Chen, Linjie Li, Licheng Yu, Ahmed El Kholy, Faisal Ahmed, Zhe Gan, Yu Cheng, and Jingjing Liu. Uniter: Universal image-text representation learning. In *European conference on computer vision*, pages 104–120. Springer, 2020.
- [9] Samyak Datta, Karan Sikka, Anirban Roy, Karuna Ahuja, Devi Parikh, and Ajay Divakaran. Align2ground: Weakly supervised phrase grounding guided by image-caption alignment. In *Proceedings of the IEEE/CVF International Conference on Computer Vision*, pages 2601–2610, 2019.
- [10] Jacob Devlin, Ming-Wei Chang, Kenton Lee, and Kristina Toutanova. Bert: Pre-training of deep bidirectional transformers for language understanding. *arXiv preprint arXiv:1810.04805*, 2018.
- [11] Alexey Dosovitskiy, Lucas Beyer, Alexander Kolesnikov, Dirk Weissenborn, Xiaohua Zhai, Thomas Unterthiner, Mostafa Dehghani, Matthias Minderer, Georg Heigold, Sylvain Gelly, et al. An image is worth 16x16 words: Transformers for image recognition at scale. *arXiv preprint arXiv:2010.11929*, 2020.
- [12] Zi-Yi Dou and Nanyun Peng. Improving pre-trained vision-and-language embeddings for phrase grounding. In *Proceedings of the 2021 Conference on Empirical Methods in Natural Language Processing*, pages 6362–6371, 2021.
- [13] Hugo Jair Escalante, Carlos A Hernández, Jesus A Gonzalez, Aurelio López-López, Manuel Montes, Eduardo F Morales, L Enrique Sucar, Luis Villaseñor, and Michael Grubinger. The segmented and annotated iapr tc-12 benchmark. *Computer vision and image understanding*, 114(4):419–428, 2010.
- [14] Zhiyuan Fang, Shu Kong, Charless Fowlkes, and Yezhou Yang. Modularized textual grounding for counterfactual resilience. In *Proceedings of the IEEE/CVF Conference on Computer Vision and Pattern Recognition*, pages 6378–6388, 2019.
- [15] Michael Grubinger, Paul Clough, Henning Müller, and Thomas Deselaers. The iapr tc-12 benchmark: A new evaluation resource for visual information systems. In *International workshop ontoImage*, volume 2, 2006.
- [16] Saurabh Gupta, Judy Hoffman, and Jitendra Malik. Cross modal distillation for supervision transfer. In *Proceedings of the IEEE conference on computer vision and pattern recognition*, pages 2827–2836, 2016.
- [17] Tanmay Gupta, Arash Vahdat, Gal Chechik, Xiaodong Yang, Jan Kautz, and Derek Hoiem. Contrastive learning for weakly supervised phrase grounding. In *European Conference on Computer Vision*, pages 752–768. Springer, 2020.
- [18] Kaiming He, Georgia Gkioxari, Piotr Dollár, and Ross Girshick. Mask r-cnn. In *Proceedings of the IEEE international conference on computer vision*, pages 2961–2969, 2017.

- [19] Zhicheng Huang, Zhaoyang Zeng, Bei Liu, Dongmei Fu, and Jianlong Fu. Pixel-bert: Aligning image pixels with text by deep multi-modal transformers. *arXiv preprint arXiv:2004.00849*, 2020.
- [20] Syed Ashar Javed, Shreyas Saxena, and Vineet Gandhi. Learning unsupervised visual grounding through semantic self-supervision. *arXiv preprint arXiv:1803.06506*, 2018.
- [21] Sahar Kazemzadeh, Vicente Ordonez, Mark Matten, and Tamara Berg. Referitgame: Referring to objects in photographs of natural scenes. In *Proceedings of the 2014 conference on empirical methods in natural language processing (EMNLP)*, pages 787–798, 2014.
- [22] Diederik P Kingma and Jimmy Ba. Adam: A method for stochastic optimization. *arXiv preprint arXiv:1412.6980*, 2014.
- [23] Ranjay Krishna, Yuke Zhu, Oliver Groth, Justin Johnson, Kenji Hata, Joshua Kravitz, Stephanie Chen, Yannis Kalantidis, Li-Jia Li, David A Shamma, et al. Visual genome: Connecting language and vision using crowdsourced dense image annotations. *International journal of computer vision*, 123(1):32–73, 2017.
- [24] Junnan Li, Ramprasaath Selvaraju, Akhilesh Gotmare, Shafiq Joty, Caiming Xiong, and Steven Chu Hong Hoi. Align before fuse: Vision and language representation learning with momentum distillation. *Advances in Neural Information Processing Systems*, 34, 2021.
- [25] Liunian Harold Li, Mark Yatskar, Da Yin, Cho-Jui Hsieh, and Kai-Wei Chang. Visualbert: A simple and performant baseline for vision and language. *arXiv preprint arXiv:1908.03557*, 2019.
- [26] Xiujun Li, Xi Yin, Chunyuan Li, Pengchuan Zhang, Xiaowei Hu, Lei Zhang, Lijuan Wang, Houdong Hu, Li Dong, Furu Wei, et al. Oscar: Object-semantics aligned pre-training for vision-language tasks. In *European Conference on Computer Vision*, pages 121–137. Springer, 2020.
- [27] Tsung-Yi Lin, Michael Maire, Serge Belongie, James Hays, Pietro Perona, Deva Ramanan, Piotr Dollár, and C Lawrence Zitnick. Microsoft coco: Common objects in context. In *European conference on computer vision*, pages 740–755. Springer, 2014.
- [28] Yongfei Liu, Bo Wan, Lin Ma, and Xuming He. Relation-aware instance refinement for weakly supervised visual grounding. In *Proceedings of the IEEE/CVF Conference on Computer Vision and Pattern Recognition*, pages 5612–5621, 2021.
- [29] Jiasen Lu, Dhruv Batra, Devi Parikh, and Stefan Lee. Vilbert: Pretraining task-agnostic visiolinguistic representations for vision-and-language tasks. *Advances in neural information processing systems*, 32, 2019.
- [30] Jiasen Lu, Vedanuj Goswami, Marcus Rohrbach, Devi Parikh, and Stefan Lee. 12-in-1: Multi-task vision and language representation learning. In *Proceedings of the IEEE/CVF Conference on Computer Vision and Pattern Recognition*, pages 10437–10446, 2020.
- [31] Tam Nguyen, Maximilian Dax, Chaithanya Kumar Mummadi, Nhung Ngo, Thi Hoai Phuong Nguyen, Zhongyu Lou, and Thomas Brox. Deepusps: Deep robust unsupervised saliency prediction via self-supervision. *Advances in Neural Information Processing Systems*, 32, 2019.
- [32] Vicente Ordonez, Girish Kulkarni, and Tamara Berg. Im2text: Describing images using 1 million captioned photographs. *Advances in neural information processing systems*, 24, 2011.
- [33] Khoi Pham, Kushal Kafle, Zhe Lin, Zhihong Ding, Scott Cohen, Quan Tran, and Abhinav Shrivastava. Learning to predict visual attributes in the wild. In *Proceedings of the IEEE/CVF Conference on Computer Vision and Pattern Recognition*, pages 13018–13028, 2021.
- [34] Vipin Pillai, Soroush Abbasi Koohpayegani, Ashley Ouligian, Dennis Fong, and Hamed Pirsiavash. Consistent explanations by contrastive learning. In *Proceedings of the IEEE/CVF Conference on Computer Vision and Pattern Recognition*, pages 10213–10222, 2022.

- [35] Bryan A Plummer, Liwei Wang, Chris M Cervantes, Juan C Caicedo, Julia Hockenmaier, and Svetlana Lazebnik. Flickr30k entities: Collecting region-to-phrase correspondences for richer image-to-sentence models. In *Proceedings of the IEEE international conference on computer vision*, pages 2641–2649, 2015.
- [36] Shaoqing Ren, Kaiming He, Ross Girshick, and Jian Sun. Faster r-cnn: Towards real-time object detection with region proposal networks. *Advances in neural information processing systems*, 28, 2015.
- [37] Anna Rohrbach, Marcus Rohrbach, Ronghang Hu, Trevor Darrell, and Bernt Schiele. Grounding of textual phrases in images by reconstruction. In *European Conference on Computer Vision*, pages 817–834. Springer, 2016.
- [38] Ramprasaath R Selvaraju, Michael Cogswell, Abhishek Das, Ramakrishna Vedantam, Devi Parikh, and Dhruv Batra. Grad-cam: Visual explanations from deep networks via gradient-based localization. In *Proceedings of the IEEE international conference on computer vision*, pages 618–626, 2017.
- [39] Ramprasaath R Selvaraju, Karan Desai, Justin Johnson, and Nikhil Naik. Casting your model: Learning to localize improves self-supervised representations. In *Proceedings of the IEEE/CVF Conference on Computer Vision and Pattern Recognition*, pages 11058–11067, 2021.
- [40] Piyush Sharma, Nan Ding, Sebastian Goodman, and Radu Soricut. Conceptual captions: A cleaned, hypernymed, image alt-text dataset for automatic image captioning. In *Proceedings of the 56th Annual Meeting of the Association for Computational Linguistics (Volume 1: Long Papers)*, pages 2556–2565, 2018.
- [41] Amanpreet Singh, Vedanuj Goswami, Vivek Natarajan, Yu Jiang, Xinlei Chen, Meet Shah, Marcus Rohrbach, Dhruv Batra, and Devi Parikh. Mmf: A multimodal framework for vision and language research, 2020.
- [42] Ashish Vaswani, Noam Shazeer, Niki Parmar, Jakob Uszkoreit, Llion Jones, Aidan N Gomez, Łukasz Kaiser, and Illia Polosukhin. Attention is all you need. *Advances in neural information processing systems*, 30, 2017.
- [43] Josiah Wang and Lucia Specia. Phrase localization without paired training examples. In *Proceedings of the IEEE/CVF International Conference on Computer Vision*, pages 4663–4672, 2019.
- [44] Liwei Wang, Jing Huang, Yin Li, Kun Xu, Zhengyuan Yang, and Dong Yu. Improving weakly supervised visual grounding by contrastive knowledge distillation. In *Proceedings of the IEEE/CVF Conference on Computer Vision and Pattern Recognition*, pages 14090–14100, 2021.
- [45] Qinxin Wang, Hao Tan, Sheng Shen, Michael W Mahoney, and Zhewei Yao. Maf: Multimodal alignment framework for weakly-supervised phrase grounding. *arXiv preprint arXiv:2010.05379*, 2020.
- [46] Tianlu Wang, Jieyu Zhao, Mark Yatskar, Kai-Wei Chang, and Vicente Ordonez. Balanced datasets are not enough: Estimating and mitigating gender bias in deep image representations. In *Proceedings of the IEEE/CVF International Conference on Computer Vision*, pages 5310–5319, 2019.
- [47] Fanyi Xiao, Leonid Sigal, and Yong Jae Lee. Weakly-supervised visual grounding of phrases with linguistic structures. In *Proceedings of the IEEE Conference on Computer Vision and Pattern Recognition*, pages 5945–5954, 2017.
- [48] Raymond Yeh, Jinjun Xiong, Wen-Mei Hwu, Minh Do, and Alexander Schwing. Interpretable and globally optimal prediction for textual grounding using image concepts. *Advances in Neural Information Processing Systems*, 30, 2017.
- [49] Raymond A Yeh, Minh N Do, and Alexander G Schwing. Unsupervised textual grounding: Linking words to image concepts. In *Proceedings of the IEEE Conference on Computer Vision and Pattern Recognition*, pages 6125–6134, 2018.

- [50] Licheng Yu, Patrick Poirson, Shan Yang, Alexander C Berg, and Tamara L Berg. Modeling context in referring expressions. In *European Conference on Computer Vision*, pages 69–85. Springer, 2016.
- [51] Licheng Yu, Zhe Lin, Xiaohui Shen, Jimei Yang, Xin Lu, Mohit Bansal, and Tamara L Berg. Mattnet: Modular attention network for referring expression comprehension. In *Proceedings of the IEEE Conference on Computer Vision and Pattern Recognition*, pages 1307–1315, 2018.
- [52] Jianming Zhang, Sarah Adel Bargal, Zhe Lin, Jonathan Brandt, Xiaohui Shen, and Stan Sclaroff. Top-down neural attention by excitation backprop. *International Journal of Computer Vision*, 126(10):1084–1102, 2018.
- [53] Fang Zhao, Jianshu Li, Jian Zhao, and Jiashi Feng. Weakly supervised phrase localization with multi-scale anchored transformer network. In *Proceedings of the IEEE Conference on Computer Vision and Pattern Recognition*, pages 5696–5705, 2018.
- [54] Jieyu Zhao, Tianlu Wang, Mark Yatskar, Vicente Ordonez, and Kai-Wei Chang. Men also like shopping: Reducing gender bias amplification using corpus-level constraints. *arXiv preprint arXiv:1707.09457*, 2017.
- [55] Bolei Zhou, Aditya Khosla, Agata Lapedriza, Aude Oliva, and Antonio Torralba. Learning deep features for discriminative localization. In *Proceedings of the IEEE conference on computer vision and pattern recognition*, pages 2921–2929, 2016.

A Supplementary

In this section we provide more details for experiments on RefCOCO+ [50] and ReferIt [21], and provide additional qualitative examples.

RefCOCO+ Clean As discussed in Anderson et al [2], there are around 51K images from Visual Genome (VG) [23] that are also present in the COCO dataset [27]. Moreover, images in the RefCOCO+ validation/testing sets come from the COCO dataset as well. While there is no overlap in the training, validation and testing sets for RefCOCO+, methods that use VG to pretrain object detectors might use some overlapping data which would make object detectors on some part of the validation and testing sets artificially accurate. In order to fully investigate whether this issue affects the generalization of previous methods, we further explore a more restricted version of the validation and test sets for RefCOCO+ so that no overlap exists with VG and re-run previous methods along with our method on this subset. After cross-referencing images in the VG training set from Anderson et al [2] and images from the RefCOCO+ validation/testing sets, we find 574 and 569 overlapping images in the RefCOCO+ validation/testing sets. In order to correct this, we also evaluate and compare our method with previous methods on a *clean* version of the RefCOCO+ validation and testing sets with 926 and 931 images respectively.

Table 4 shows that in fact this overlap did not have much of an effect on previous methods – and our method also performs at a high accuracy. Our method still outperforms VMRM [12] and InfoGround [17] by a large margin. We also report results for ALBEF [24] and compare it with InfoGround and VMRM which uses bounding boxes for object detectors during training. Even though ALBEF does not use any box information, it still achieves good performance on the RefCOCO+ dataset. Our method, which uses box information, can further improve the pointing accuracy results under both settings.

Box Recall Evaluation We use pointing accuracy because this metric has been previously used in both detector-based [17] and detector-free [3, 1] methods. Another metric that can be considered is *Recall@k* from detector-based methods [17, 12]. For *Recall@k*, the model will rank all the box proposals generated by an object detector, and select the top-k boxes as results. If a selected box and the ground truth box have an intersection over union (IoU) ≥ 0.5 , the selected box will be counted as positive. Table 5 shows results when we evaluate our method by using it to choose boxes from different bounding box proposals methods by selecting the boxes with high attention heatmap scores. We use boxes generated by the FasterRCNN [36] from Gupta et al [17] and the MaskRCNN [18] from Yu et al [51]. Using the MaskRCNN proposals, our method obtains consistently better results than VMRM, which is the current stats-of-the-art. However, we find this metric is influenced by the quality of boxes. For example, using the MaskRCNN proposals will get much better results than using the FasterRCNN proposals for VMRM [12].

Sample Spatial Prompts In our main paper, we discuss how to construct textual descriptions using bounding boxes and attributes. In Figure 3, we show several examples of such constructed data. In total, we generate 924, 807 text descriptions using attributes and 168, 442 descriptions with spatial references.

Method	RefCOCO+‡		RefCOCO+§	
	test A	test B	test A	test B
InfoGround [17]	39.80	41.11	40.10	40.62
VMRM [12]	58.87	50.32	60.29	50.39
ALBEF [24]	69.37	53.77	69.40	54.04
AMC	80.34	64.55	80.33	65.02

Table 4: We show pointing accuracy results on the RefCOCO+ validation and testing sets with original and clean images. ‡ indicates original image splits and § indicates splits with clean images.

Method	Box	RefCOCO+	
		test A	test B
VMRM [12]	FasterRCNN	30.04	30.78
VMRM [12]	MaskRCNN	46.63	40.52
ALBEF [24]	MaskRCNN	61.70	42.83
AMC	MaskRCNN	68.04	46.55

Table 5: We show recall@1 results on the RefCOCO+ validation and testing sets.



Figure 3: We show some constructed textual descriptions with colored attributes and spatial references.

Qualitative Results Figure 4 shows additional qualitative results on the test set of RefCOCO+ and Figure 5 shows similar qualitative results for ReferIt.



Figure 4: We show more qualitative examples for the RefCOCO+ testing set. Ground truth boxes are marked as red boxes. Below each image we provide with one input phrase.

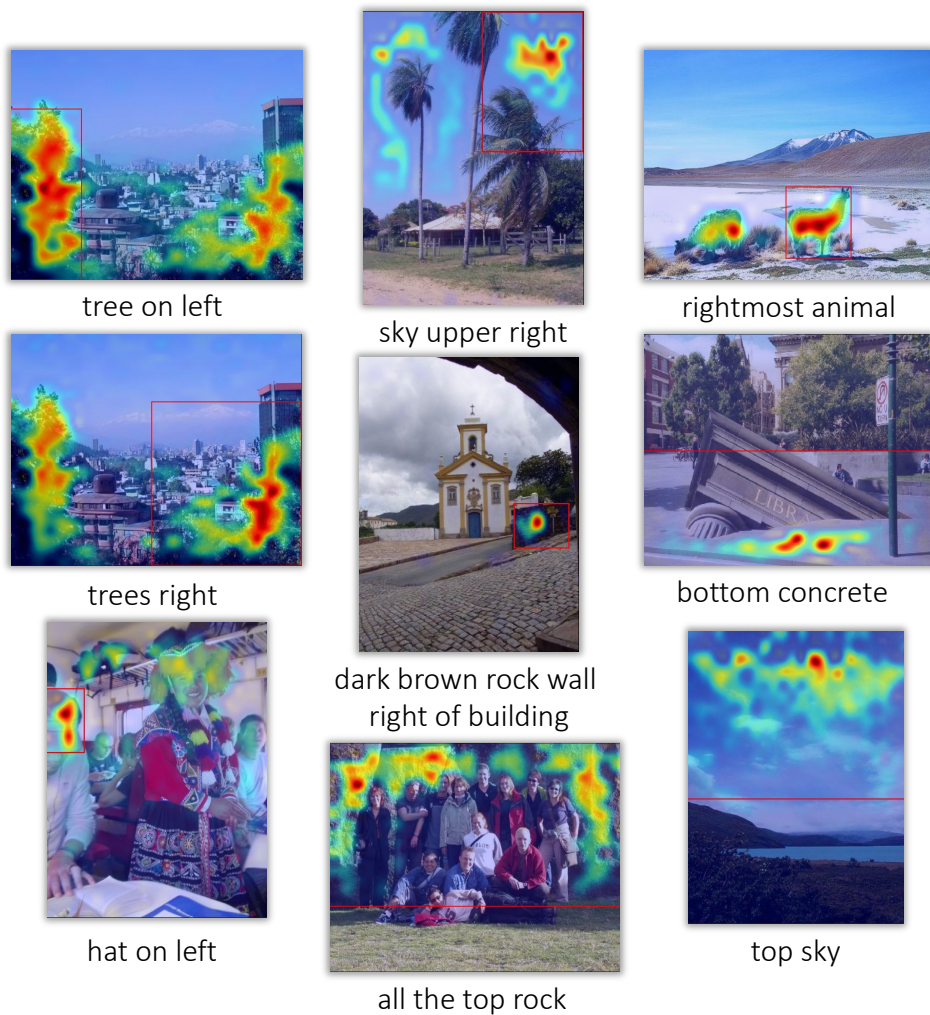


Figure 5: We show more qualitative examples for the ReferIt testing set. Ground truth boxes are marked as red boxes. Below each image we provide with one input phrase.